Journal of Advanced Chemical Engineering
ISSN: 2090-4568

Okon et al., J Adv Chem Eng 2016, 6:2
DOI: 10.4172/2090-4568.1000147

Research Article Open Access

Evaluation and Characterisation of Composite Mesoporous Membrane for Lactic Acid and Ethanol Esterification

Edidiong Okon, Habiba Shehu and Edward Gobina*

Center for Process Integration and Membrane Technology (CPIMT), School of Engineering, The Robert Gordon University, Aberdeen, AB10 7GJ, United Kingdom

Abstract

Recently, the use of inorganic composite mesoporous membranes in chemical industries has received a lot of attention due to a number of exceptional advantages including thermal stability and robustness. Inorganic mesoporous membranes can selectively remove water from the reaction product during lactic esterification reactions in order to enhance product yield. In this work, the characterization and evaluation of a catalytic mesoporous membrane with 15 nm pore size was tested with different carrier gases before employing the gases for lactic acid and ethanol esterification product analysis with Gas Chromatography coupled with mass spectrometry (GC-MS). The membrane was coated once with silica solution before the permeation test with carrier gases. Helium (He), nitrogen (N_2), argon (Ar) and carbon dioxide (CO_2) were used for the permeation tests conducted at the feed pressure of 0.10–1.00 bar and at the temperature of 413 K. The gas flow rate showed an increase with respect to feed pressure indicating Knudsen flow as the dominant transport mechanism. The order of the gas flow rate with respect to the feed pressure drop was Ar>CO_2>He>N_2. The morphological characteristic of the membrane was determined using scanning electron microscopy coupled with energy dispersive x-ray analyzer (SEM/EDXA). The SEM result of the membrane showed the distribution of the silica on the surface of the membrane. The surface area and pore size distribution of the silica membrane was analyze using liquid nitrogen adsorption/desorption method. The surface area results obtained from the Brunauer-Emmett-Teller (BET) isotherm for the 1st and 2nd dip-coated membranes were 1.497 and 0.253 m^2/g whereas the Barrette-Joyner-Halenda (BJH) curves for the pore size of the 1st and 2nd dip-coated membranes were 4.184 and 4.180 nm respectively, corresponding to a mesoporous structure in the range of 2-50 nm. The BET isotherms of the silica membranes showed a type IV isotherm with hysteresis. The BJH curve for the 2nd dip-coated membrane showed a 4% reduction in pore size after the modification process.

Keywords: Characterisation; Permeation; Inorganic membrane; Esterification; Gas transport; Isotherm

Introduction

Solvents play a major role in all stages of industrial manufacturing sector. The environmental and toxicological effects of solvents have become important in chemical processes. Because environmental problems have threatened the natural order including climate change and global warming, a lot of research is being carried out to find environmentally safe chemicals and processes [1]. Lactic acid is the simplest hydroxycarboxylic acid with an asymmetric carbon atom. It can be obtained from biomass, petroleum and coal. Copolymers and polymers of lactic acid are known to be eco-friendly and are compatible due to their degradability mild products, which makes them desirable as an alternative petrochemical polymer [2]. Lactic acid can react with ethanol during esterification process to produce ethyl lactate which is used as flavour chemicals, food additive, perfumery and as solvent. Ethyl lactate can replace environmentally damaging solvents including toluene, acetone, N-methyl pyrrolidone and xylene [3]. The use of inorganic ceramic membrane to selectively eliminate water from the reaction product during esterification of lactic acid is yet another important application that has attracted a lot of attention [4]. Membrane-based separation technologies have shown a wide range of application in food, biotechnology, pharmaceutical and in the treatment of other industrial effluents [5].

Membrane may be classified as heterogeneous or homogeneous, asymmetric or symmetric, solid or liquid, charged or uncharged and organic or inorganic membranes. The types of membranes include: dense, porous and composite membranes. They can also be inorganic and organic membranes. Table 1 shows the classification of inorganic membrane base on their nature and their most essential characteristics, permeability and selectivity [6]. Inorganic membranes have shown an increasing interest in the separation of gas mixtures at high temperatures. However, one of the most promising uses of inorganic membrane is in the reactors where product purification by separation and chemical conversion occurs in the same device resulting in process intensification. Moreover, it is possible to obtain important enhancement over the equilibrium conversion of the reactor feed stream by selectively separating one or more reaction products across the membrane wall [7]. The function of the porous membrane during esterification reaction is to selectively remove water from the reaction mixture which will result in an equilibrium shift thus, driving the reaction towards completion [8,9]. Membranes different geometry and characteristics are generally made from a wide variety of chemically and thermally stable polymers. Other materials including alumina, titania, zirconia and silica are also being used [6].

Inorganic membrane can be prepared using different methods including sol-gel, chemical vapour deposition and sintering methods. Sol-gel method of preparation has been found to be the most suitable method for porous membrane preparation in contrast to chemical vapour deposition and sintering methods [10]. The mechanism of gas transport through membranes is generally divided into 5 groups: surface

***Corresponding author:** Edward Gobina, Center for Process Integration and Membrane Technology (CPIMT), School of Engineering, The Robert Gordon University, Aberdeen, AB10 7GJ, United Kingdom, Tel: +44(0)1224262348; E-mail: e.gobina@rgu.ac.uk

Received February 11, 2016; **Accepted** March 18, 2016; **Published** March 25, 2016

Citation: Okon E, Shehu H, Gobina E (2016) Evaluation and Characterisation of Composite Mesoporous Membrane for Lactic Acid and Ethanol Esterification. J Adv Chem Eng 6: 147. doi:10.4172/2090-4568.1000147

Types of membrane	Material	Permeability	Selectivity
Composite	Metal-metal	Moderate	Very selective
	Ceramic-metal		
Dense	Metallic	Low/moderate	High
	Solid-electrolyte		
Porous	Microporous	Moderate	Very selective
	Mesoporous	Moderate/high	Low/moderate
	Macroporous	high	Non-selective

Table 1: Summary of the classification of inorganic membrane.

diffusion, capillary condensation, Knudsen diffusion, viscous flow and molecular sieving mechanisms [11]. In Knudsen diffusion mechanism, gas molecules diffuse through the pores of the membrane and then get transported by colliding more frequently with the pore walls. Viscous flow mechanism takes place if the pore radius of the membrane is larger than the mean free path of the permeating gas molecule. Gas separation by molecular sieving mechanism takes place when the pore dimensions of the inorganic ceramic membrane approach those of the permeating gas molecules [12]. However, in capillary condensation mechanism, separation can takes place in the pores of the membrane with mesoporous layer in the presence of condensable gas specie [12].

Surface diffusion mechanism occurs when the adsorption of the permeating gas molecule occurs on the pore surface of the membrane material there by increasing the gas transport performance [12]. Physisorption is known as one of the most important method to characterised nanosized porous material with respect to the pore volume, pore size distribution and specific surface area [13]. According to Lee et al. [14], when the gas molecule interacts with the solid surface, the amount of the gas molecule adsorbs on the surface equals the total partial pressure of the gas molecule. However, the measurement of the adsorbed amount of gas over a range of partial pressure at a single temperature produces an adsorption isotherm. Hence, the resulting adsorption isotherm shows the various types based on the pore structure of a porous media and intermolecular interaction between the gas molecule and the surface [14].

According to IUPAC (International Union of Pure and Applied Chemistry), the physisorption isotherm can be classified into six different types as explained below:

• Type I isotherm is characterised by the adsorption in the non-porous microporous region at a low relative pressure.

• Type II is characteristic of non-porous or macroporous adsorbents with the formation of a multilayer of adsorbate (gas molecule) on the surface of the adsorbent (membrane material).

• Type III is characteristic by a non-porous or macroporous layer with weak interaction between the gas molecule and the membrane material.

• Type IV isotherm reflects a macroporous material which involves the coverage of the monolayer-multilayer on the external and mesoporous surface which is followed by capillary condensation in the mesoporous region with the formation of several hysteresis loop based on the shape of the pores.

• Type V isotherm is characteristic of a mesoporous material and involves the weak interaction between the permeating gas molecule and the membrane material.

• Type VI isotherm takes place in a highly uniform surface [13]. During the specific surface area analysis of the internal and external surface of porous material using physical gas adsorption, the amount of gas adsorbed depends on the relative vapour pressure [13].

In this study, the characterisation and evaluation of a mesoporous composite membrane with 15 nm pore size was investigated to determine the permeation properties of carrier gases (Ar, He, N_2 and CO_2) with the composite membrane before lactic acid and ethanol esterification reactions process.

Experimental

Permeation tests

The four carrier gases used for the permeation analysis include; nitrogen (N_2), argon (Ar), helium (He) and carbon dioxide (CO_2). The gases were supplied by BOC, UK. The permeation analysis was carried out at the feed pressure drop of 0.10–1.00 bar and at 413 K. The porous tube support was modified once before the permeation analysis. The total length of the membrane was 36.6 cm, while the inner and outer radius of the membrane was 7 and 10 mm respectively. The support modification process was carried out based on the procedure developed by Gobina [15]. Figure 1 shows the single gas permeation setup [16].

Liquid nitrogen adsorption

The surface area analysis of the support and coated support was examined using liquid nitrogen adsorption instrument, prior to the analysis, a small fragment of the silica membrane was crushed and used for the liquid nitrogen analysis. The actual weight of the 1st and 2nd dipping membrane samples was 4.3 g and 4.2 g respectively. The sample cells weight for the 1st and 2nd dipping was 16.8 g and 27.7 g respectively. The degassing of the system was carried out using a flow of a dry helium gas with some heat in order to remove moisture from the sample. A similar procedure to that of Vospernik et al. [17] was use for the liquid nitrogen analysis with some modification in the temperature. The liquid nitrogen temperature was 77 K.

The actual weights of the silica membranes, the cell weight and the weight of sample + cell before and after the degasing process are presented in Table 2. The pictorial diagram of the liquid nitrogen adsorption instrument is shown in Figure 2.

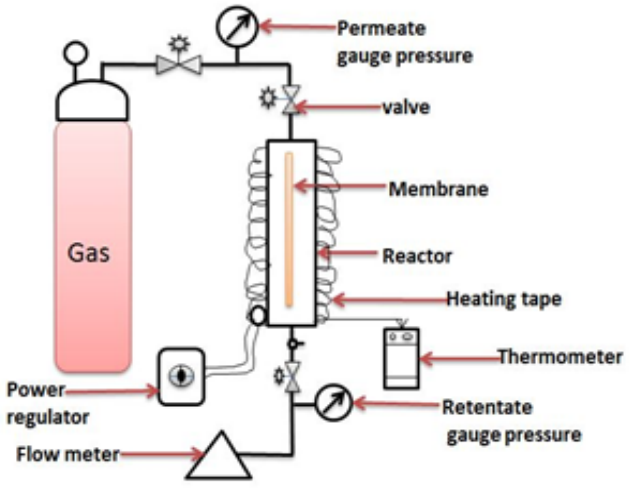

Figure 1: Schematic diagram of gas permeation setup.

Sample	Cell weight (g)	Weight of sample+cell before degasing(g)	Actual weight of sample (g)	Weight of sample after degasing (g)
1st dipping	16.8	21.1	4.3	21.0
2nd dipping	27.7	31.9	4.2	31.8
Support	16.8	21.1	4.2	21.0

Table 2: Sample and cell weights before and after degasing process.

Results and Discussion

Figure 3 shows the relationship between the gas flow rate (mol/sec) and the feed pressure drop (bar) at 413 K. From the result obtained, it was found that the gas flow rate increase with respect to feed pressure (bar). The order of the gas flow rate through the silica membrane as shown in Figure 3 was: Ar (40 mol/g)>CO_2 (44 mol/g)>He (4 mol/g)>N_2 (28 mol/g). It can be seen that Ar gas showed a higher flow than CO_2 with the highest molecular weight. However, N_2 gas with the higher molecular weight showed a higher flow in contrast to He gas with a least molecular weight. According to Knudsen flow mechanism, gases with the least molecular weight can permeate faster than gases with the heavier molecular weight. It was found that the order of gas flow rate was not based on the Knudsen flow mechanism of transport which as a relationship with the gas molecular weight. From the gas flow rate relation with the feed pressure drop, Ar gas was suggested as the suitable carrier and detector gas to be coupled with GC-MS for the analysis of the esterification lactic acid and ethanol esterification product.

Figure 4 shows the relationship between the gas flow rate ($mols^{-1}$) and the inverse square root of the gas molecular weight. According to Markovic et al. [18], Knudsen diffusion is the dominant flow mechanism of transport in silica membrane if gas flow rate is proportional to the inverse square root of the gas molecular weight. From the result obtained in Figure 4, it was observed that there was no linear proportionality correlation of the gases with the inverse square root of the molecular weight indicating that the Knudsen flow mechanism was non-operative.

The relationship between the gas permeance and inverse of the gas viscosity was also plotted at the gauge pressure drop of 0.9 bar and 413 K. From Figure 5, it was observed that gases with highest viscosity value showed the least permeance which suggests that the gas flow through the silica membrane was based on viscous flow mechanism of gas transport.

From the result obtained in Table 2, it was observed that the sample weight reduced in size by 0.1 g in both silica membrane samples after the degasing process. The BET and BJH of the two membrane samples were obtained from the liquid nitrogen adsorption. The amount of the adsorbed gas molecule depends on the relative vapour pressure (P/P_O). Figures 6 and 7 shows the plot of the amount of gas adsorbed (volume at STP (cc/g)) against the relative pressure P/P_O for the 1st and 2nd dip-coated fragments. The BET isotherm of the both membranes possess hysteresis loop in their curves indicating the pore size of 4.184 nm for the 1st dip-coated fragment and 4.180 for the 2nd dip- coated fragment respectively as shown in Table 3. The pore size of the dip-coated silica membranes was characteristic of mesoporous structure with hysteresis which was indicative of a capillary condensation in the mesoporous region.

From Figure 6, the nitrogen adsorption isotherm for the 1st dip-coated membrane was observed to be similar to that of a type IV physisorption isotherm with the presence of hysteresis based on the six classification of the BET isotherm. A similar result was obtained by Lee et al. [7]. Comparing the BET isotherms of the 1st and 2nd dip-coated membranes, it was observed that the hysteresis in the BET curve of the 1st dip-coated fragment was higher compared to the 2nd dip-coated fragment. This was due to the fact that the 1st dip-coated membrane exhibited a higher surface area and pore size before the dip-coating process however, hysteresis effect decreases after each dipping process which was also attributed to the reduction in the pore size of the membrane.

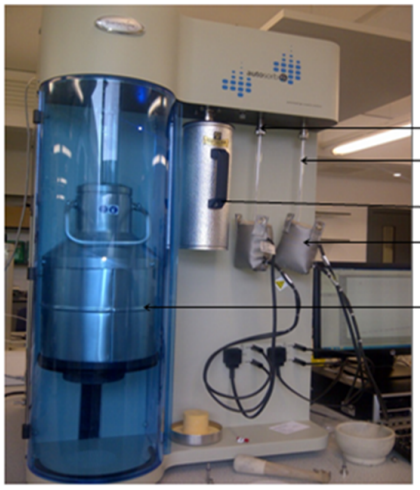

Figure 2: Pictorial diagram of the Liquid Nitrogen adsorption at the Centre for Process Integration and Membrane Technology (CPIMT), RGU.

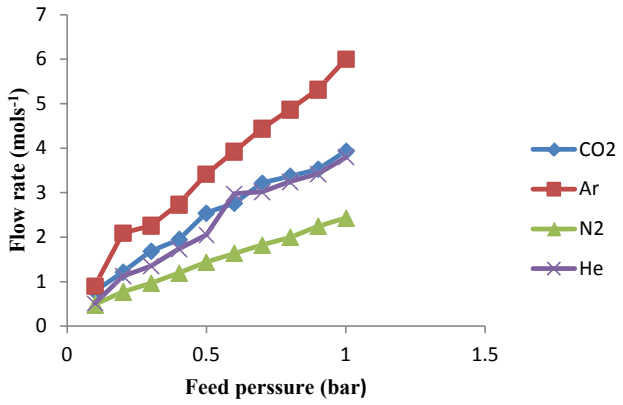

Figure 3: Relationship between gas flow rate (mol/sec) and the feed pressure drop (bar) and 413 K.

	BET	BJH	
Sample	Surface area (m^2/g)	Pore diameter(nm)	Pore Volume (cc/g)
1st dipping	0.253	4.184	0.006
2nd dipping	1.497	4.180	0.004

Table 3: BET and BJH values for 1st and 2nd dip-coated silica membrane.

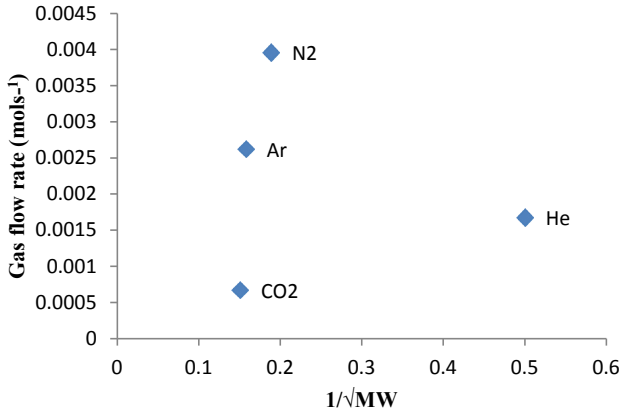

Figure 4: Relationship between the gas flow rate (mols^{-1}) and inverse square root of gas molecular weight at 0.90 bar and 413 K.

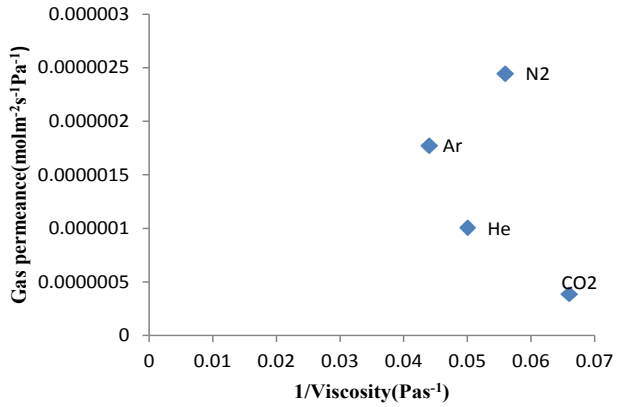

Figure 5: Gas permeance against 1/viscosity (Pas^{-1}) at 0.9 bar gauge pressure (bar) and 413 K.

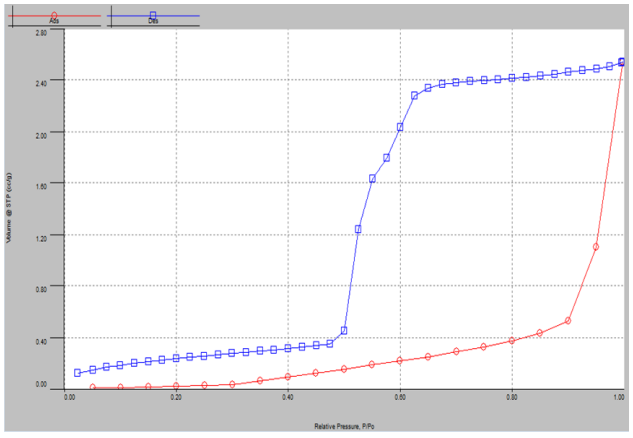

Figure 6: BET isotherm for the 1st dip-coated membrane.

The pore size distribution for the silica material was estimated based on the BJH results. From Figure 8, it was observed that the silica membrane showed a mesoporous structure with the pore diameter and pore volume of 4.184 nm and 0.006 cc/g respectively for the 1st dip-coated membrane whereas the pore diameter and the pore volume of the 2nd dipping from Figure 9 were 4.180 nm and 0.004 cc/g respectively.

However, the surface area of the 1st dip-coated membrane was found to be lower in contrast to the 2nd dip-coated membrane and shown in Table 2. It was observed that there was a 4% reduction in the pore diameter of the membrane after the dipping process, which confirmed the fact that the membrane was characteristic of a mesoporous structure and the silica membrane was suitable for gas molecules to penetrate through the pore walls. A similar result was obtained by Markovic et al. [18].

The surface of the silica membrane was examined using Scanning electron microscopy and energy dispersive x-ray analyser (SEM-EDXA) to determine the structural morphology of the membrane sample. From Figure 10, it was found that a defect-free surface with no evidence of crack on the surface of the silica membrane. It was also found that the silica solution was distributed evenly on the surface of the membrane.

Conclusion

The gas transport across silica membrane was not entirely based by Knudsen mechanism of transport but included other mechanism such as viscous flow. The gas flow rate showed an increase with respect to feed pressure drop. The SEM image of the silica membrane showed a clear surface without any crack on the surface. The BET of the 1st and 2nd coated silica membrane showed a type IV isotherm with the presence of hysteresis in both curves, indicating that the membrane

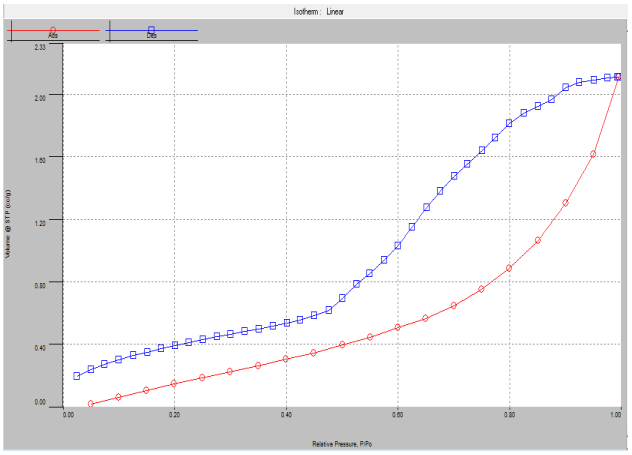

Figure 7: BET isotherm for the 2nd dip-coated membrane.

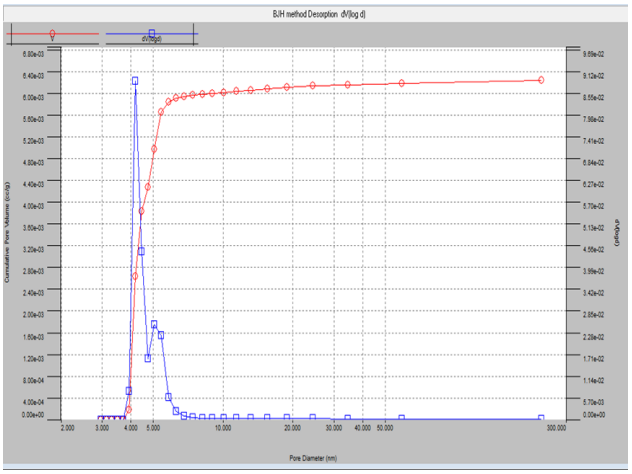

Figure 8: BJH curve for 1st dip-coated membrane.

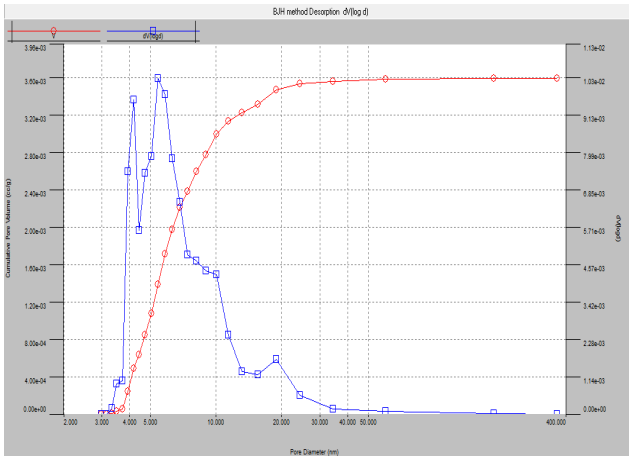

Figure 9: BJH curve for 2nd dip-coated membrane.

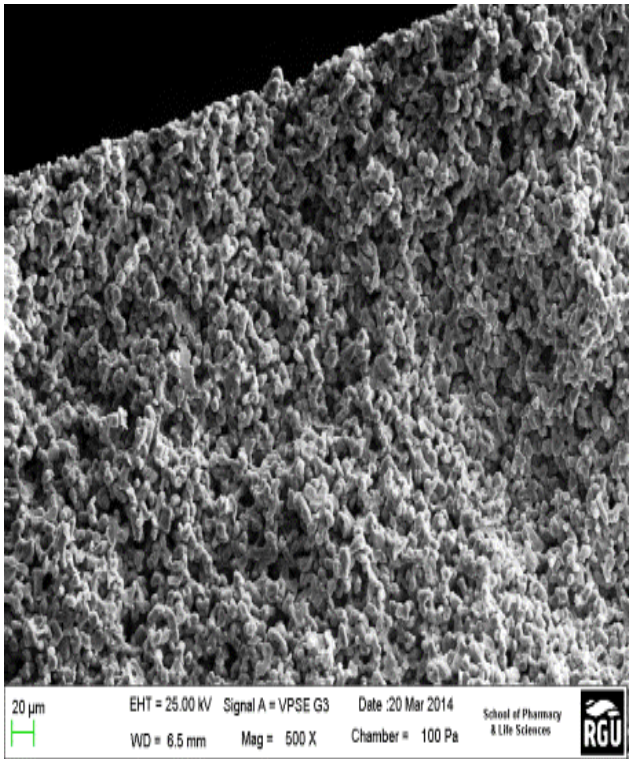

Figure 10: SEM surface image of cross-section of the silica membrane.

was characteristic of a mesoporous classification in the range of 2-50 nm. The hysteresis in the BET isotherm of the 1st dip-coated membrane was found to be larger than that of the 2nd dip-coated membrane indicating the effect of the dip-coating process. The BJH of 2nd coated silica membranes showed an average pore reduction of 4% after the modification process.

Acknowledgments

The authors wishes to express sincere thanks to and CPIMT for supplying the membrane and other infrastructures used in the study, School of Pharmacy and Life Science, RGU for the SEM images. Additionally, CCEMC is great fully acknowledged for their financial contribution towards the research work.

References

1. Nigiz FU, Hilmioglu ND (2015) Green solvent synthesis from biomass based source by biocatalytic membrane reactor. International Journal of Energy Research 40: 71-80.
2. Sanz MT, Murga R, Beltrán S, Cabezas JL, Coca J (2004) Kinetic study for the reactive system of lactic acid esterification with methanol: Methyl lactate hydrolysis reaction. Industrial & Engineering Chemistry Research 43: 2049-2053.
3. Engin A, Haluk H, Gurkan K (2003) Production of lactic acid esters catalyzed by heteropoly acid supported over ion-exchange resins. Green Chemistry 5: 460-466.
4. Pereira CS, Silva VM, Rodrigues AE (2011) Ethyl lactate as a solvent: Properties, applications and production processes-a review. Green Chemistry 13: 2658-2671.
5. Calvo JI, Bottino A, Capannelli G, Hernández A (2008) Pore size distribution of ceramic UF membranes by liquid–liquid displacement porosimetry. J Memb Sci 310: 531-538.
6. Mulder M (1996) Basic Principles of Membrane Technology. Kluwer Academic Publishers, The Netherlands.
7. Collins JP, Way JD (1993) Preparation and characterization of a composite palladium-ceramic membrane. Industrial & Engineering Chemistry Research 32: 3006-3013.
8. Zhang Y, Ma L, Yang J (2004) Kinetics of esterification of lactic acid with ethanol catalyzed by cation-exchange resins. React Funct Polym 61: 101-114.
9. Dassy S, Wiame H, Thyrion FC (1994) Kinetics of the liquid phase synthesis and hydrolysis of butyl lactate catalysed by cation exchange resin. J Chem Technol Biotechnol 59: 149-156.
10. Ju X, Huang P, Xu N, Shi J (2000) Influences of sol and phase stability on the structure and performance of mesoporous zirconia membranes. J Memb Sci 166: 41-50.
11. Abedini R, Nezhadmoghadam A (2010) Application of Membrane in Gas Separation Processes: Its Suitability and Mechanisms. Petroleum & Coal 52: 69-80.
12. Lee H, Suda H, Haraya K (2005) Gas permeation properties in a composite mesoporous alumina ceramic membrane. Korean J Chem Eng 22: 721-728.
13. Weidenthaler C (2011) Pitfalls in the characterization of nanoporous and nanosized materials. Nanoscale 3: 792-810.
14. Lee H, Yamauchi H, Suda H, Haraya K (2006) Influence of adsorption on the gas permeation performances in the mesoporous alumina ceramic membrane. Sep Purif Technol 49: 49-55.
15. Gobina E (2006) Apparatus and Method for separating gases. United States patent. Patent No.7048778 B2, Robert Gordon University, Aberdeen, UK.
16. Okon E, Shehu H, Gobina E (2014) Synthesis of Gas Transport through Nano Composite Ceramic Membrane for Esterification and Volatile Organic Compound Separations. Journal of Mechanics Energy and Automation 4: 905-913.
17. Vospernik M, Pintar A, Bercic G, Batista J, Levec J (2004) Potentials of Ceramic Membranes as Catalytic Three-Phase Reactors. Chemical Engineering Research and Design 82: 659-666.
18. Markovic A, Stoltenberg D, Enke D, Schlünder E, Seidel-Morgenstern A (2009) Gas permeation through porous glass membranes: Part I. Mesoporous glasses-effect of pore diameter and surface properties. J Memb Sci 336: 17-31.